COMITATO NAZIONALE PER L'ENERGIA NUCLEARE
Laboratori Nazionali di Frascati

LNF - 66/20
20 Marzo 1966

C. Bacci, C. Mencuccini, G. Penso, G. Salvini, and V. Silvestrini: # PHOTOPRODUCTION CROSS SECTION FOR INCIDENT PHOTON ENERGIES 800 TO 1000 MeV. -

(Nota interna: n. 318)

Servizio Documentazione
dei Laboratori Nazionali di Frascati del CNEN
Casella Postale 70 - Frascati (Roma)

Laboratori Nazionali di Frascati del CNEN
Servizio Documentazione

LNF-66/20

Nota interna: n. 318
29 Marzo 1966

C. Bacci(x), C. Mencuccini, G. Penso(x), G. Salvini(x), V. Silvestrini: η PHOTOPRODUCTION CROSS SECTION FOR INCIDENT PHOTON ENERGIES 800 TO 1000 MeV.

(Submitted for publication to il Nuovo Cimento)

SUMMARY -

Photoproduction cross-section of the η particle for incident photon energies K from $\sim$800 to $\sim$1000 MeV has been measured at the 1.1 GeV Frascati electronsynchrotron.

The differential cross section for this process, at c.m. angle of the η of $\sim 110^{o}$, turns out to be fairly constant for 830 MeV $\leq K \leq$ 900 MeV, and drops down of a factor 5 to 10 at K = 950 MeV. These results are discussed in terms of a comparison with the data on the production of η's by pions, and with the data on pion-nucleon scattering and pion photoproduction.

The conclusions are in agreement with the hypothesis that the η-N system is dominated at low energies by a resonance with orbital angular momentum 1 = 0 ($S_{1/2,1/2}$ resonance).

(x) - Istituto di Fisica dell'Università di Roma and Istituto Nazionale di Fisica Nucleare, Roma

INTRODUCTION -

In this paper we describe an experiment which has been carried out during last year at the 1.1 GeV Frascati electronsynchrotron, in order to measure the differential cross section for photoproduction of the η -particle in the reaction

(1) $$\gamma + p \rightarrow \eta + p$$

The experimental results have been already synthetically presented elsewhere[1].

In section 1 we describe the experimental lay-out. The criteria used in the analysis of the data are discussed in section 2. The experimental results are presented in section 3, along with a discussion of the possible sources of errors. In section 4 we compare our results with the results on η production by pions, as well as with pion-nucleon scattering and pion photoproduction. Our conclusions are presented in section 5.

SECTION 1: EXPERIMENTAL ARRANGEMENT -

The experimental lay-out is shown in fig. 1. It is similar in principle to the one used in our previous experiment[2], which has been de-

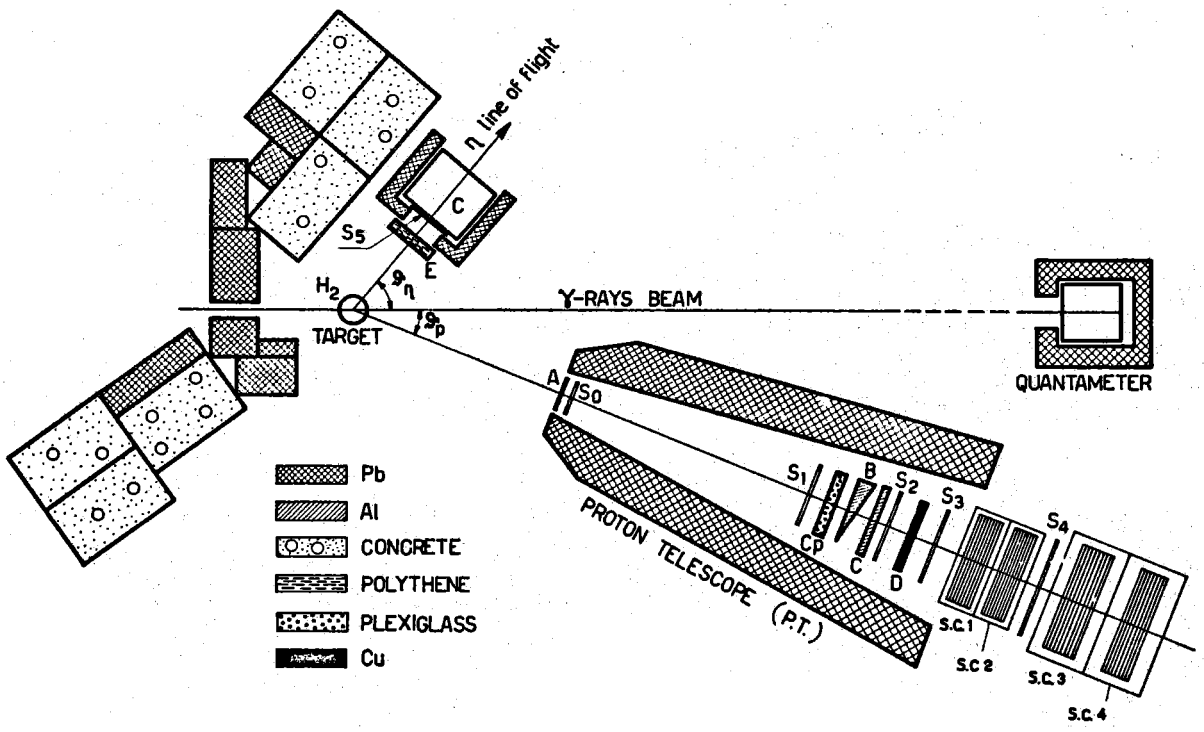

FIG. 1 - Experimental lay-out (see table I)

scribed in detail in ref. 3, but it has now a much larger acceptance and better resolution.

The main point in our arrangement is to detect the recoil proton in the proton telescope P.T. (measuring its angle and energy), and the γ-rays from neutral decays of the η in the Cerenkov C (measuring their energy).

The Cerenkov C is set on the line of flight of the η. The kinematical situation with the specific values of θ_p (angle of emission of the proton in the lab.) and θ^*_η (angle of emission of the η in the c.m.s.) is given in fig. 2.

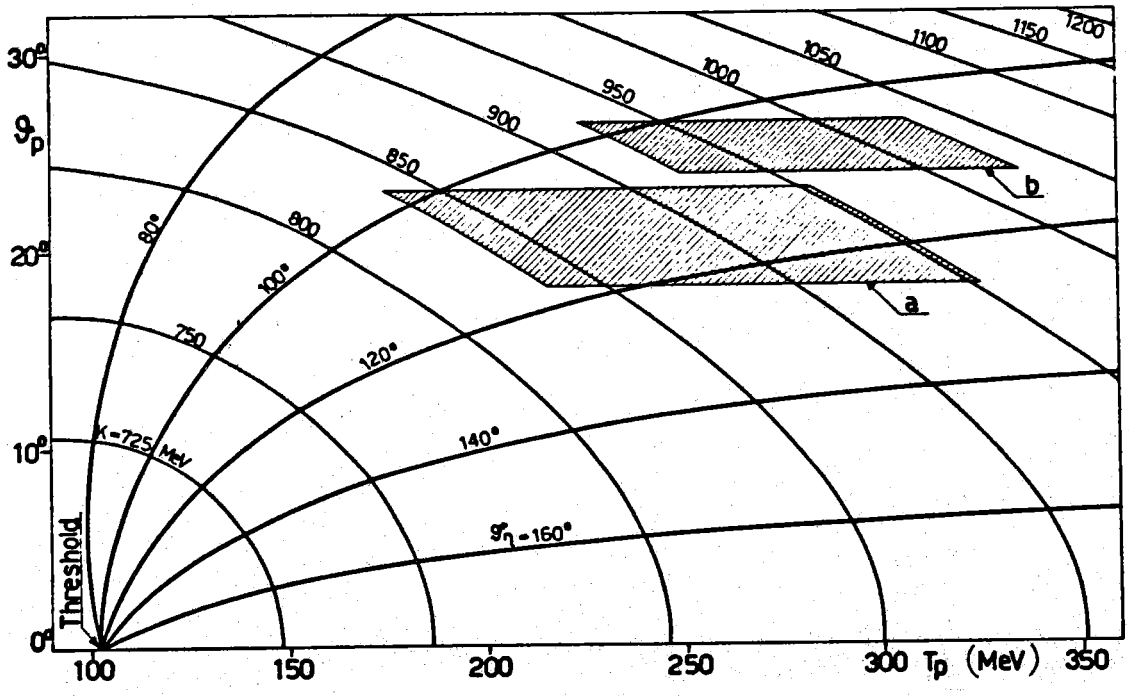

FIG. 2 - Kinematics of reaction (1): Lab. proton angle (θ_p) vs. Lab. proton kinetic energy (T_p). Curves parameters: incident photon Lab. energy (K) and c. m. angle of the η (θ^*_η). The shaded areas represent the kinematical situations chosen in the present (a), and in our previous[2] experiment (b).

The γ-rays beam from the Frascati 1.1 GeV electronsynchrotron is incident upon a 7.4 cm liquid hydrogen target[4]. The proton telescope (fig. 1) consists in the scintillators S_0 to S_4, the plexiglass Cerenkov Counter Cp, and the four spark chambers S.C.1 to S.C.4. This telescope measures the energy of the recoil protons through their range in the spark chambers, and discriminates against pions and electrons. The γ-telescope (total absorption lead glass Cerenkov counter C with an anticoincidence S_5 in front) which detects γ-rays in coincidence with the protons, measures their energy through the pulse height.

The proton telescope, the γ-ray telescope and the block diagram of the electronics are described in the following. A list of the characteristics of counters, absorbers and spark chambers is given in table I.

TABLE I

Characteristics of counters and absorbers

Distance from H_2 target (cm)	Counter or absorber (fig. 1)	Material	Dimensions	Phototubes N° Type
PROTON TELESCOPE				
98	A	Al plate	8 mm thick	
100	S_o	plastic scintillator	15x15x0.5 cm^3	1 Philips 56AVP
215	S_1	plastic scintillator	23x23x1.25 cm^3	1 Philips 56AVP
225	Cp	plexiglass Cerenkov	25x25x5.6 cm^3	4 Philips 56AVP
235	B	Al wedge	12 mm medium thickness	
245	C	Al plate	adjustable thickness	
249	S_2	plastic scintillator	23x23x2.5 cm^3	2 Philips 56AVP
259	D	Cu plate	3 mm thick	
269	S_3	plastic scintillator	22x22x1 cm^3	1 Philips 56AVP
282 (first plate)	S.C.1+S.C.2	(13+13) Al plates (Spark chambers)	(13+13)(31.5x31.5x0.3cm^3)	
315	S_4	plastic scintillator	35x35x1.2 cm^3	1 Philips 56AVP
330 (first plate)	S.C.3+S.C.4	(13+13) Al plates (Spark chambers)	(13+13)(41.5x41.5x0.3cm^3)	
γ-RAY TELESCOPE				
35	E	Polythene	25 cm diameter 6 cm thick	
45	S_5	Plastic scintillator	27x27x1.2 cm^3	1 Philips-56 AVP
50	C	lead glass cylinder (total absorption Cerenkov)	30 cm diameter 25 cm thick	3 Philips 58 AVP

a) The proton telescope.

The proton telescope (fig. 1) is centered at an angle $\theta_p = 20.6^o$ with respect to the incident photon beam direction and has an angular acceptance $\Delta\theta_p = \pm 2.4^o$ corresponding to a solid angle, defined by counter S_3, of 6.7 msr in the laboratory system.

The elements of the proton telescope are:

S_0, S_1, S_2, S_3, S_4: scintillation counters;

Cp : plexiglass Cerenkov counter;

S.C. : spark chambers;

A, B, C, : aluminum absorbers

D : copper absorber

The spark chambers[5] are sandwiches of aluminium plates (3 mm thick), and glass frames (5.5 mm thick) glued with araldit. Henogal gas mixture (65% Neon, 35% Helium) is circulated in each chamber. A hole in each aluminum plate, at opposite corners for neighbouring plates, allows gas circulation through the all chamber. Each chamber has 13 aluminum plates (12 gaps); S.C.1 and S.C.2 are 31,5 x 31,5 cm^2; S.C.3 and S.C.4 are 41,5 x 41,5 cm^2 useful area.

The spark chambers are driven by four spark-gaps in air, which are triggered when a coincidence of a "proton" with a γ-ray in C occurs.

A "proton" is defined by the coincidences:

$$N_1 = S_0(S_1D)S_2S_3\bar{S}_4 \quad \text{or} \quad N_2 = S_0S_1S_2S_3S_4\bar{C}p$$

$\bar{S}_4$ and $\bar{C}p$ being in anticoincidence. (S_1D) means a discrimination on the pulse height of the counter S_1.

The triggering through N_1 or N_2 guarantees that all the protons stopping in the four spark chambers are counted. In fact N_2 are particles entering S.C.3 and S.C.4 (fig. 1). Since pions and electrons entering S.C.3 and S.C.4 are above the Cerenkov threshold in Cp, there is only a small contamination of them in N_2.

Conversely, pions stopping in S.C.1 and S.C.2 are often below threshold in Cp, which therefore has not been used in N_1. The discrimination on S_1, however, eliminates a good percentage of pions stopping in S.C.1 and S.C.2 without eliminating protons. The additional condition of a coincidence with a γ-ray in C, reduces to $\sim$ 10% the contamination of pions in the triggers of the spark chambers. Finally, the pulse heights in S_2 and S_3 are digitized and recorded on each photo: complete elimination of pions is then allowed, when analysing the data, by a two-dimensional pulse height plot for particles stopping in a small range interval (fig. 3).

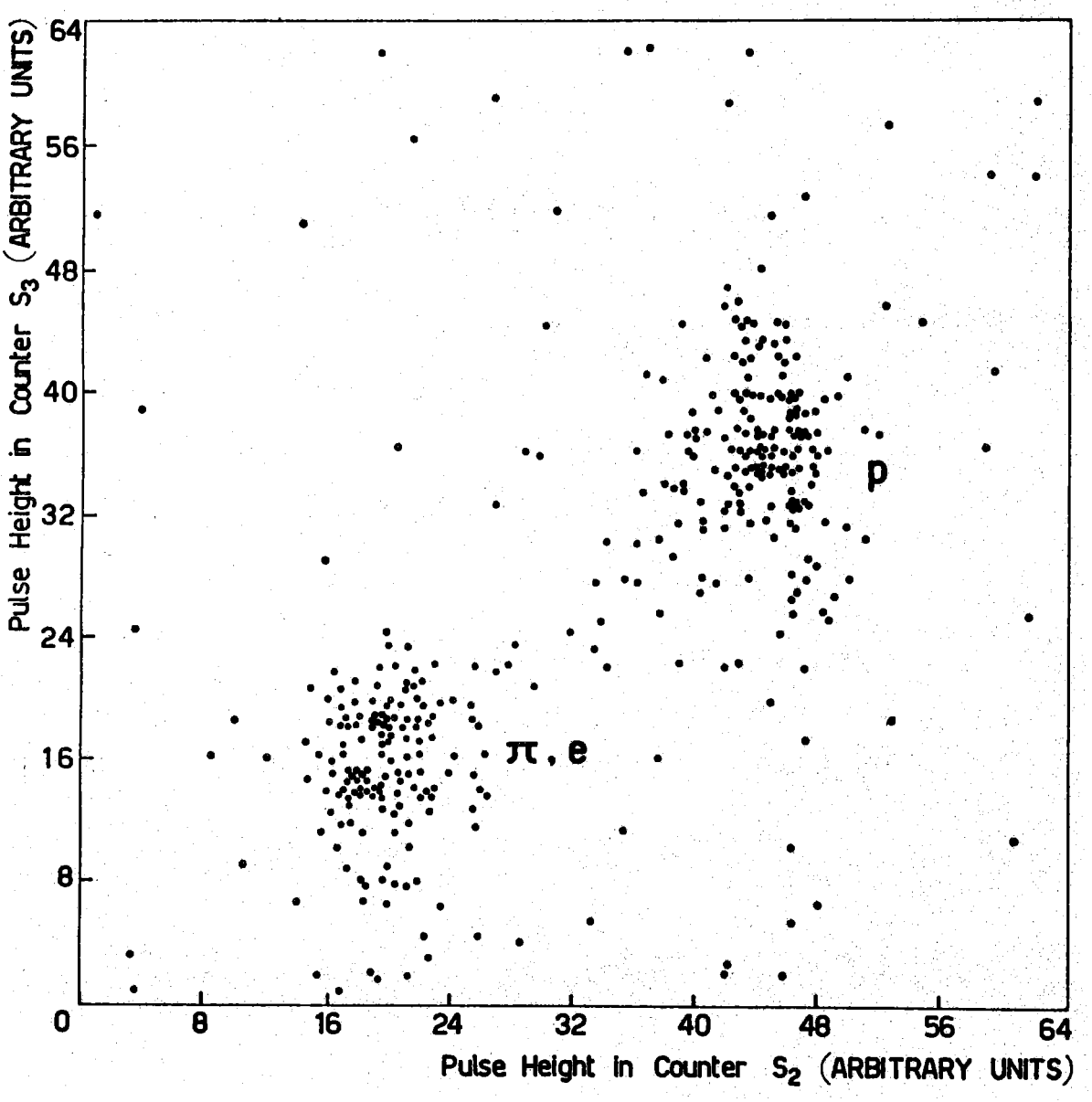

FIG. 3 - Bidimensional plot of pulse heights in counters S_2 and S_3. Protons are clearly separated from electrons and pions.

The wedge aluminum absorber B in P.T. corrects for the dependence of the energy of the recoil protons from reaction (1) on their angle of emission. This allows a one to one correspondence between the energy of the incident photon an the stopping gap of the proton in S.C., simplifying the analysis of the data.

b) The γ-ray telescope.

The total absorption Cerenkov counter C (fig. 1) is a cylinder (30 cm in diameter, 25 cm thick) of lead glass manufactured by Shott (Jena), 60% in weight of Pb, with a radiation length of $\sim$2.5 cm; it is viewed by three 58AVP phototubes.

The container of the phototubes, with their voltage dividers, is cooled with forced air circulation to avoid drifts due to changes in temperature.

A lead collimator in front of C (fig. 1) reduces the useful area to 25 cm in diameter. The anticoincidence counter S_5 is placed between the lead collimator and the Cerenkov. A slab of polythene 6 cm thick shields S_5 from low energy particles, to lower the rate of accidental anticoincidences.

The Cerenkov counter C was calibrated using monochromatic electrons from the Frascati pair spectrometer[6]. The result of the calibration (pulse height analyser channel vs. electron energy) is shown in fig. 4.

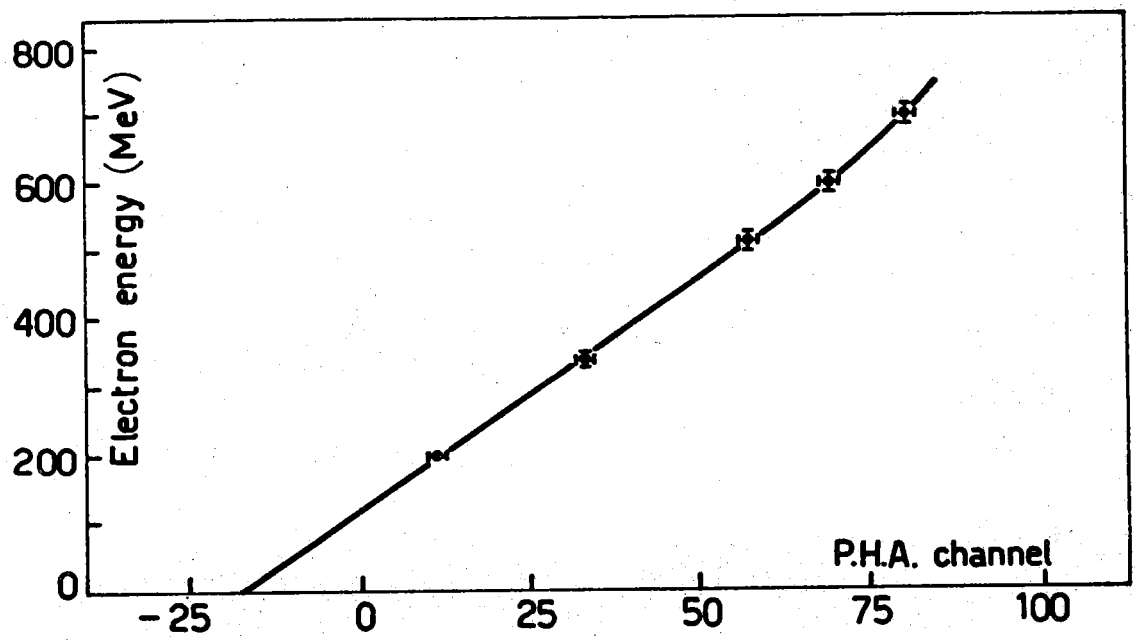

FIG. 4 - Results of the calibration of the lead glass Cerenkov C: energy of incident electrons (MeV) vs. average pulse height analyzer channel.

The resolution during the calibration turned out to be $\sim \pm 20\%$ (half width at half maximum) at 500 MeV, changing as $\sim 1/\sqrt{E}$ with the electron energy.

c) The electronics.

The block diagram of the electronics is shown in fig. 5. Most of the elements used are described in ref. 7. The part concerning the coincidence between the proton channel and the γ-ray channel has been duplicated in order to have a simultaneous measurement of the accidental rate which is, for the coincidence γ-proton, as high as $\sim 10\%$. The accidental rate in the proton channel is much smaller (~ 2-3%).

The pulse height spectrum of the Cerenkov counter C is measured in a multichannel analyser: the digitized output of the analyser is

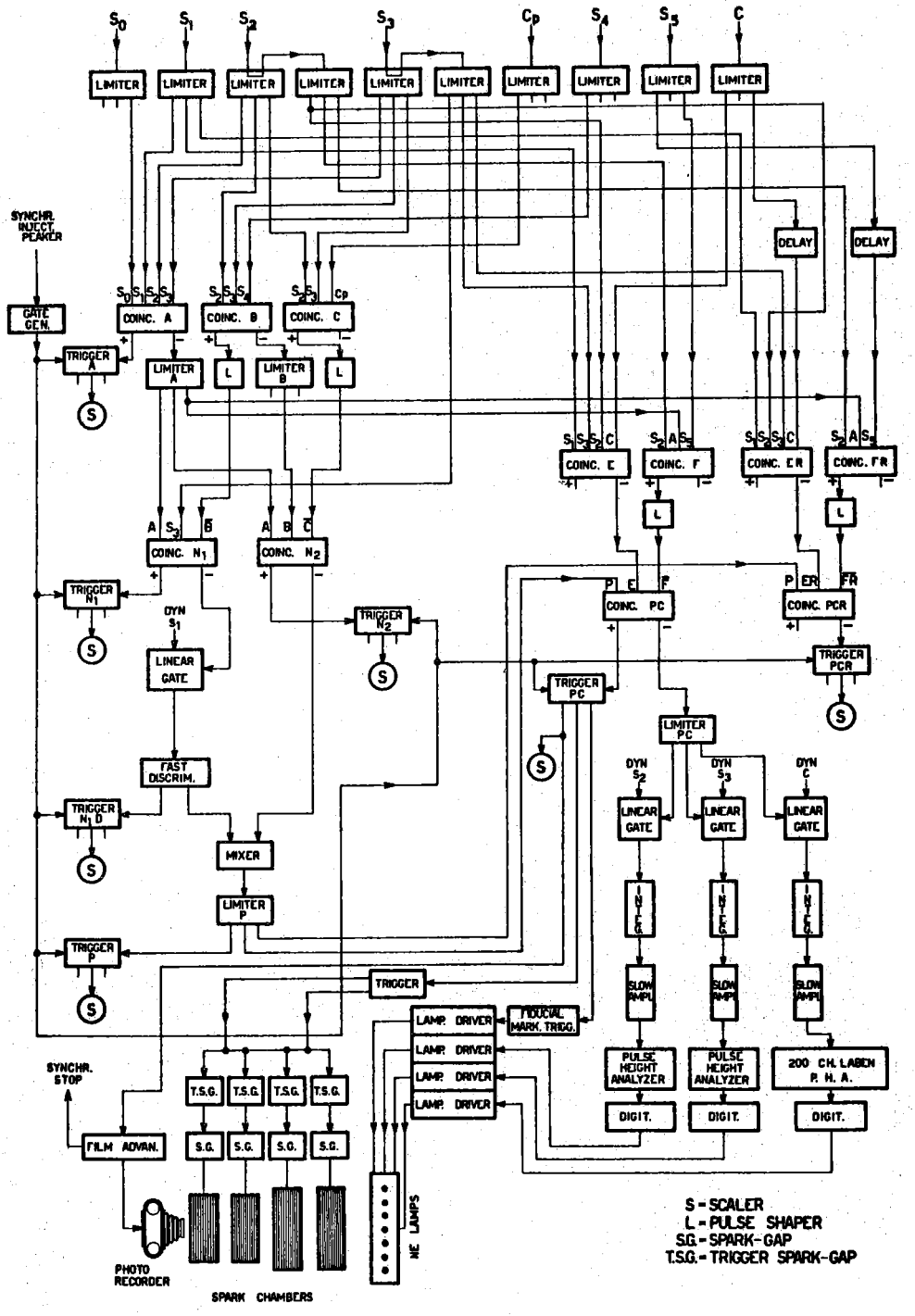

FIG. 5 - Block diagram of the electronics.

also recorded on each photo, which thus contains the following informations: angle and energy of the proton from the spark chambers: we use the Berkeley range-energy tables[8] to get the kinetic energy of the proton; energy of the γ-ray in the Cerenkov C; pulse heights in S_2 and S_3.

SECTION 2: DATA REDUCTION -

After the elimination of pions and electrons from the particles detected in P.T. our information is summarized in a bidimensional plot, whose coordinates are: the stopping-gap of the proton, that is a quantity which goes with the kinetic energy T_p of the proton; and the multichannel response to the Cerenkov C, that is a quantity going with the energy E_γ of the detected photon. When we project this plot on the proton axis, we obtain the proton energy spectrum (fig. 6); when we

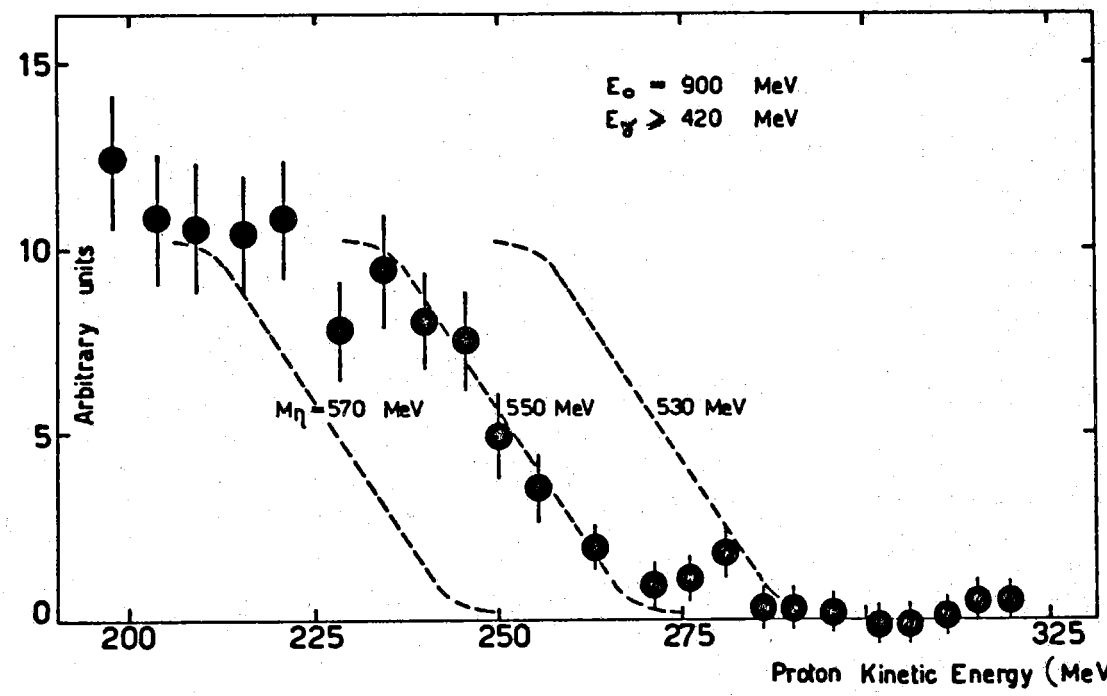

FIG. 6 - A typical result of the step method: energy spectrum of protons in coincidence with a γ-ray in C with energy $E_\gamma \geq 420$ MeV. The step characteristic of recoil protons from reaction (1) is clearly visible, overposed to a small background. The expected position of the step for different values of the mass of the η is shown. The machine energy (E_o) was 900 MeV.

project on the γ-ray axis, we get the energy distribution of the γ's (fig. 7).

Both the photon spectra and the proton spectra contain useful information on reaction (1).

a) γ-ray spectra.

The η can undergo at least the following decay modes:

$\eta \to \pi^+\pi^-\gamma$ $\qquad$ $\eta \to \gamma\gamma$ $\qquad$ $\eta \to \pi^o\gamma\gamma$

$\eta \to \pi^+\pi^-\pi^o$ $\qquad$ $\eta \to 3\pi^o$

The expected energy spectra of photons entering C from the neutral decay modes of the η are shown in fig. 8. They have been compu-

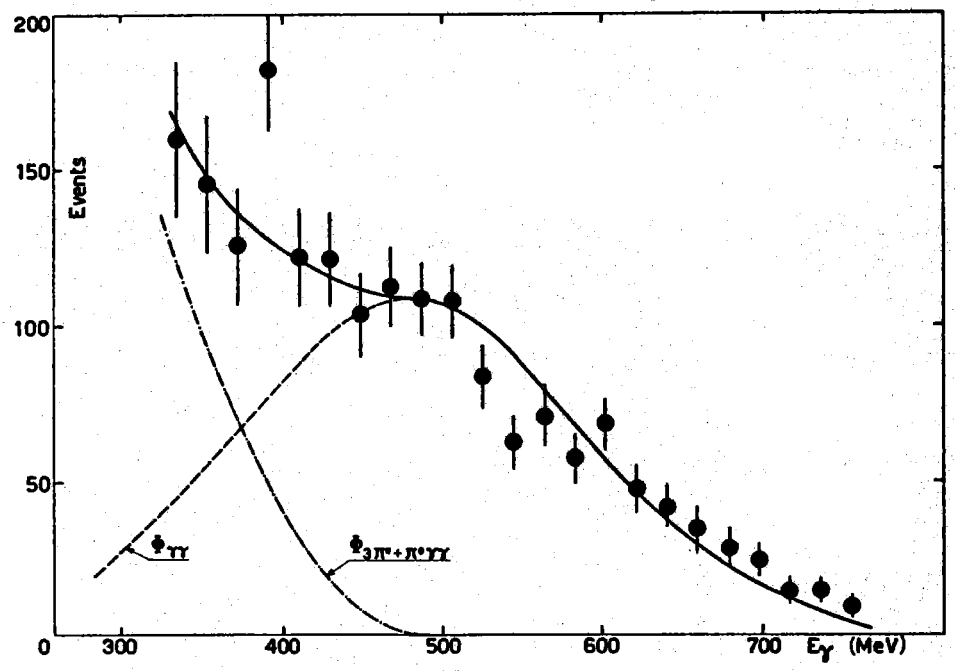

FIG. 7 - Result of the γ-ray method: energy spectrum of photons in C in coincidence with protons whose energy was compatible with being recoil protons from reaction (1). The spectrum is fitted with the expected shape for photons from the neutral decays of the η.

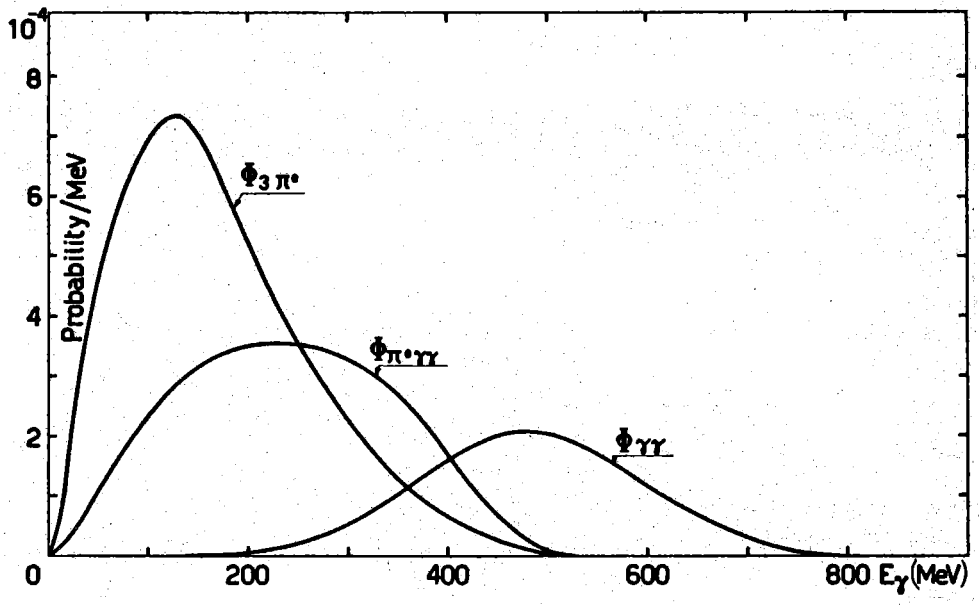

FIG. 8 - γ-ray energy spectra in C expected from the decays of the η. The calculation has been done in the statistical model. Experimental resolution folded-in. For spectra normalization see text.

ted in the statistical model, using Monte Carlo method. The finite dimensions of the counters and the energy resolution of the Cerenkov C have been taken into account.

The spectra are normalized to equal probability for the different decay modes. Therefore the area

$$\int_0^\infty \phi_i(E_\gamma)dE_\gamma$$

represents the efficiency of detection in C of the i-th decay mode (i stands for $\gamma\gamma$, $3\pi^o$, $\pi^o\gamma\gamma$). As we see, the spectrum due to the decay mode $\eta \rightarrow \gamma\gamma$ is quite different from the others: it is a peak whose width is determined practically only by the energy resolution of C and centered at an energy of 480 MeV, where the contribution from the other decay modes is rather small. The contribution from background processes (multipion production) is very similar to the contribution from the decay $\eta \rightarrow 3\pi^o$. The spectra of fig. 8 refer to an incident photon energy K = 900 MeV, but they are quite insensitive to this parameter. Once an experimental E_γ-spectrum has been collected (referring to protons stopping in a small range interval, that is to a small K interval), the number of events due to reaction

(1') $$\gamma + p \rightarrow \eta + p \quad (\eta \rightarrow \gamma\gamma)$$

can be extracted by fitting the spectrum with the curves of fig. 8. This method is not very satisfactory, due to the rather poor resolution of the Cerenkov C. However, the results we got are in very good agreement with the results of the more powerful step method, which we are going to describe.

b) Proton spectra.

The energy spectrum of protons from reaction (1) is expected to be an image of the bremsstrahlung spectrum, wheighted with the cross-section for process (1). Therefore it must show a step, corresponding to the end of the bremsstrahlung spectrum. The height of this step over the smooth spectrum of protons from background processes is proportional to the cross section for process (1). The main difficulty of this method is that the step is generally very small, over the total contribution of background processes.

However, if we select protons in coincidence with high energy photons in the Cerenkov C (for instance $E_\gamma \geq 420$ MeV), it is clear from the spectra of fig. 8 that not very much is left but the contribution of process (1'). In fact, we get in this case proton spectra which are very close to pure steps, the contribution from background processes being quite small.

This background has been evaluated on the following line: by collecting experimental data at many different values of the machine energy (E_o), a sistematic investigation of background processes is performed in the kinematical region just below threshold of η production at our angle. We then extrapolate in the region where the η is produced as described in detail in ref. 3. It is worth noticing however that the multipion background is less important in this experiment than in our previous one[2], since in the chosen kinematical region the cross section for reaction (1) turned out to be a factor 5 to 10 higher than before, the multipion background being almost unchanged.

SECTION 3: EXPERIMENTAL RESULTS -

a) Step method.

A tipical proton spectrum in coincidence with photons in the Cerenkov counter of energy $\geq$ 420 MeV, is shown in fig. 6. The expected position of the step for different values of the mass of the η is also shown. As we see, the background from other processes than process (1) is indeed very small. In fig. 9 the difference between two proton spectra corresponding to different energies E_o of the electronsynchrotron (900 MeV and 860 MeV) is given. In this case, the spectrum is a peak, whose position corresponds to a mass of the η of 550 MeV, with an error of a few MeV. The absolute calibration of the machine energy, and of the energy scale in the proton spectrum, was checked by making a similar step-spectrum from single π^o photoproduction[3].

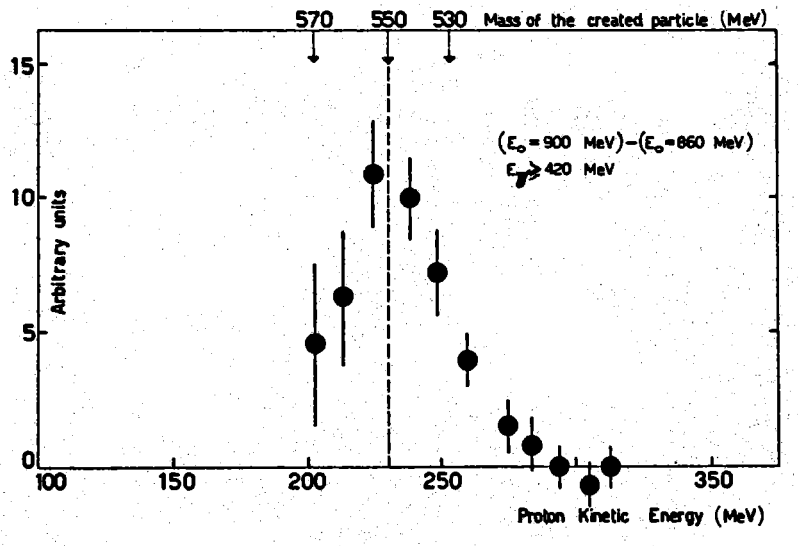

FIG. 9 - Typical result of the differentiation method: difference between two proton energy spectra (in coincidence with photons of energy $E_\gamma \geq$ $\geq$ 420 MeV in C) taken at different values of the machine energy (E_o = = 900 MeV and E_o = 860 MeV). The expected position of the peak for different values of the mass of the η is shown (upper scale).

From the various spectra of the type shown in fig. 6 one can calculate the cross section for process (1):

$$\frac{d\sigma}{d\Omega^*} = \frac{n}{\varepsilon} \frac{\varepsilon_1 \varepsilon_2}{N_{H_2} N_\gamma \Delta\Omega^*} \tag{2}$$

where

$\frac{d\sigma}{d\Omega^*}$ is the c.m. differential cross section relative to a given c.m. angle θ^*_η of emission of the η in reaction (1);

n is the number of η events observed in a given energy interval of the incident photons;

ε is the efficiency of detection of the η through its decay products. ε can of course be calculated once the spectra of fig. 8 are known. The main source of error in ε comes from a possible error in the absolute calibration of C, affecting the energy cut-off at a nominal value of 420 MeV. A possible error of $\pm$ 7% in the energy calibration was propagated to ε.
A factor ($\sim$ 0.94) was applied to the efficiency to correct for the absorption of γ-rays in the polythene in front of S_5.

N_{H_2} is the number of protons per cm^2 in the H_2 target. From the geometry of the liquid hydrogen target, N_{H_2} was evaluated with an estimated error of $\pm$ 3%.

$\varepsilon_1 \varepsilon_2$ are correction terms which take into account the nuclear interactions and the Coulomb scattering in P.T., respectively. ε_1 was evaluated using a mean free path for interaction in aluminum λ = = 110 g/cm^2, as extracted from Millburn et al[11]. A possible error of $\pm$ 20% in λ was propagated to ε_1. ε_2 was evaluated to be $\sim$ 1 in our telescope.

$\Delta\Omega^* = \frac{d\Omega^*}{d\Omega} \Delta\Omega$ is the c.m. solid angle of the proton telescope. It was calculated from the geometry of the telescope, and checked by making a distribution of the events as a function of the entrance point in the spark chamber (fig. 10). This checks also that $\varepsilon_2 \simeq 1$.

N_γ is the number of incident photons in the concerned energy interval.

We have:

$$N_\gamma = \frac{1}{K} b\left(\frac{K}{E_o}\right) \Delta K \, Q$$

where:

$\frac{1}{K} b\left(\frac{K}{E_o}\right)$ is the energy spectrum of the bremsstrahlung beam[9]

$\Delta K = \frac{dK}{dT_p} \Delta T_p$ is the accepted energy interval of the incident photon;

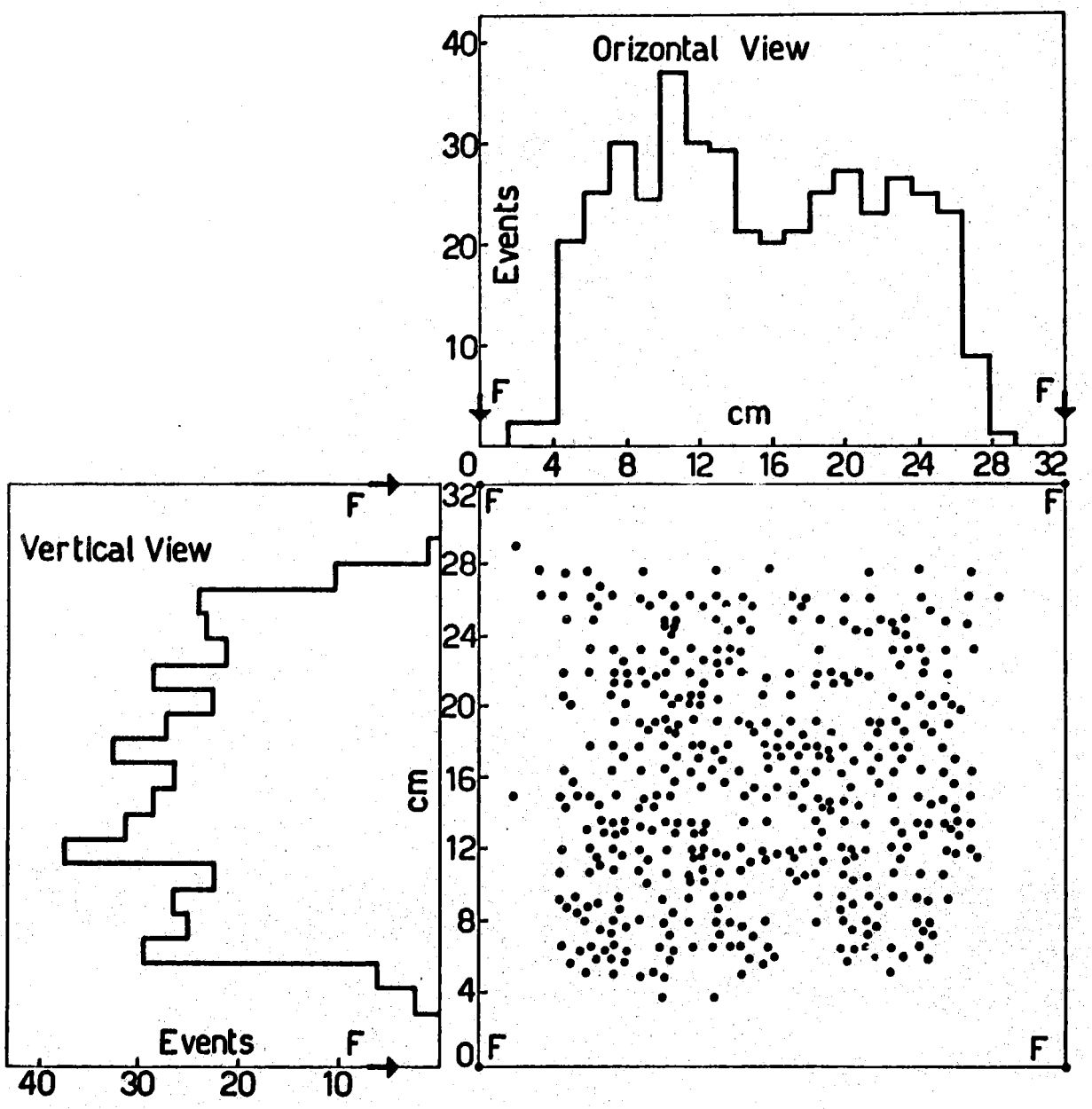

FIG. 10 - Distribution of protons entering S.C.1 as a function of the entrance coordinates. This distribution fits well with the shadow from the H_2 target of counter S_3, which defines the solid angle. The fiducial marks F indicate the useful area of the spark chambers.

K is the average value of the energy of the accepted incident photons;
Q is the number of equivalent quanta measured with a Wilson quantameter[10];
N_γ was considered known with an error of $\pm$ 5%, due to a possible error in the calibration of the Wilson quantameter;

b) γ-rays method.

As we said, the number of events $\eta \to \gamma\gamma$ is extracted from the γ-ray spectra by fitting the experimental spectra with the computed spectra of fig. 8. The cross-section is then computed on the same lines as for the step method.

The results of the two methods are clearly not statistically independent. The consistency of the results obtained with the two methods (fig. 11), checks against systematic errors in the extraction of η -events from background.

c) Results.

In table II (column 2) the results for the cross section $(d\sigma/d\Omega^*)$ $(\eta \to \gamma\gamma)$ are given (step method). In table III the values of the cross section from the analysis of the γ-spectra are also given.

The values of the cross section $(d\sigma/d\Omega^*)$ for the process

$$\gamma + p \to \eta + p \quad (\eta \to \text{all modes})$$

reported in table II (column 3), are obtained by dividing the measured cross section for $\gamma + p \to \eta + p$, $(\eta \to \gamma\gamma)$ by the branching ratio

$$\frac{\eta \to \gamma\gamma}{\eta \to \text{all modes}} ,$$

which is known from the world average[12] as 0.38 ± 0.03.

In fig. 11 we report $(d\sigma/d\Omega^*)(\eta \to \gamma\gamma)$ (ordinates on the left) and $(d\sigma/d\Omega^*)(\eta \to$ all modes) (ordinates on the right).

In table IV the photon flux used to collect each set of data is reported in equivalent quanta.

SECTION 4: DISCUSSION OF OUR RESULTS AND COMPARISON WITH OTHER DATA. -

A) - Let us first make some immediate comment on our values of the cross section, reported in fig. 11. The cross section at least at our angles, goes down rather drastically from K = 850 MeV to 950 MeV. We

TABLE II

Differential cross sections for the process $\gamma + p \rightarrow \eta + p$ as obtained with the step method.

Col.(1): energy of the incident γ-ray, laboratory system.

Col.(2): differential cross section in the c.m.s. relative to the η decaying in the mode $\eta \rightarrow \gamma\gamma$.

Col.(3): differential cross section in the c.m.s. for $\eta \rightarrow$ all modes ($\Gamma_{\gamma\gamma}/\Gamma_{TOT} = 0.38$ from the world average[12]).

Col.(4): Center of mass angle of the η.

(1)	(2)	(3)	(4)
K (MeV)	$(d\sigma/d\Omega^*)_{\gamma\gamma}$ $(10^{-31}cm^2/sr)$	$(d\sigma/d\Omega^*)$ $(10^{-31}cm^2/sr)$	θ^*_η (deg.)
836	4.24 ± 0.51	11.1 ± 1.3	107
841	3.29 ± 0.51	8.7 ± 1.3	108
847	4.05 ± 0.59	10.7 ± 1.5	109
853	3.71 ± 0.59	9.8 ± 1.5	110
859	4.05 ± 0.59	10.7 ± 1.5	111
866	4.14 ± 0.51	10.8 ± 1.3	112
873	4.05 ± 0.59	10.7 ± 1.5	113
879	3.04 ± 0.59	8.0 ± 1.5	113
884	3.37 ± 0.76	8.8 ± 2.0	114
889	3.04 ± 0.76	8.0 ± 2.0	114
895	3.46 ± 0.76	9.1 ± 2.0	115
905	2.36 ± 0.42	6.2 ± 1.1	115
915	1.35 ± 0.59	3.5 ± 1.5	116
921	1.35 ± 0.68	3.5 ± 1.8	116
926	2.23 ± 1.30	5.9 ± 3.4	117
932	1.95 ± 1.30	5.1 ± 3.4	117
937	2.14 ± 1.40	5.6 ± 3.7	118
944	0.65 ± 0.84	1.7 ± 2.2	118
950	0.28 ± 0.93	0.74 ± 2.4	119
955	0.56 ± 1.02	1.5 ± 2.7	119

TABLE III

Differential cross section for the process $\gamma + p \rightarrow \eta + p$ (γ-rays method). For symbols see table I.

(1)	(2)	(3)
K (MeV)	$(d\sigma/d\Omega^*)_{\gamma\gamma}$ $(10^{-31} cm^2/sr)$	$(d\sigma/d\Omega^*)$ $(10^{-31} cm^2/sr)$
839 ± 8	3.38 ± 0.61	8.9 ± 1.6
857 ± 10	3.73 ± 0.63	9.8 ± 2.6
889 ± 21.5	3.13 ± 0.50	8.2 ± 2.2
927 ± 17.4	1.73 ± 0.47	4.6 ± 1.2

TABLE IV

Photon flux used to collect the data. Different values of the machine energy were set during the measurements, in order to get a good evaluation of multipion background.

Machine energy E_o (MeV)	Number of equivalent quanta
810	$18.6 \cdot 10^{12}$
860	20.0 "
900	31.0 "
940	40.0 "
980	19.9 "

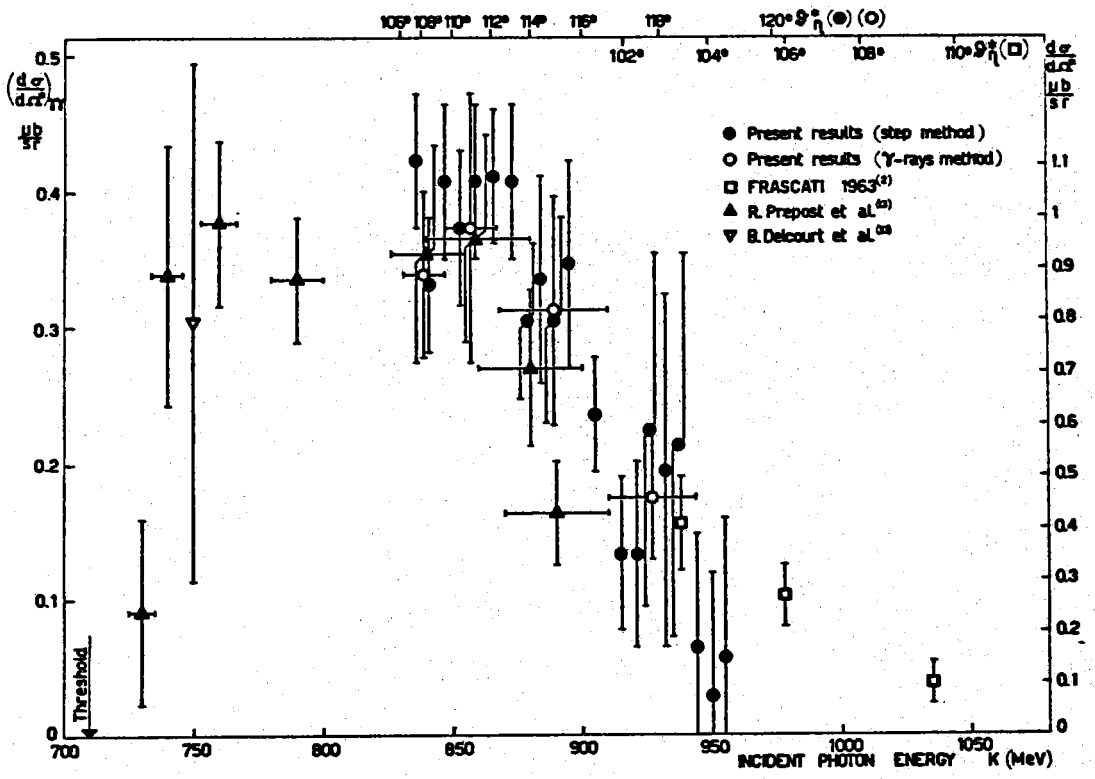

FIG. 11 - Experimental results on η-photoproduction cross section around 90° c.m.s., available up to now.

know from the work of Prepost et al.[13] that the cross section for process (1) arises from threshold (710 MeV) rather abruptly and stays more or less at the same values from ~760 MeV to ~860 MeV. Prepost et al[13] also found that the cross section is rather close to isotropy at ~ 800 MeV.

The photoproduction of the η has therefore a fast rise and a rather fast decrease, which immediately invites to look for a resonant behaviour, or at least for the large phase-shift responsible for this anomaly.

This question goes to the fundamental aspects of the η-baryon system: in fact a similar behaviour (fast rise and rather fast descent), even if not so pronounced, is observed in the reaction $\pi^- + p \rightarrow \eta + n$ by Bulos et al[14]. Beyond this, such a behaviour of the η cross section appears in a dramatic way in the $\eta\Lambda$ system[15]. In fact in the reaction $K^- + p \rightarrow \eta + \Lambda$ the total cross section reaches its maximum at ~ 5 MeV above the threshold in the c.m.s. (this corresponds to a c.m. momentum of ~ 50 MeV/c) and is again below one half of the maximum at ~ 25 MeV above the threshold (that is about 140 MeV/c of the η c.m. momentum).

The η seems therefore ready to appear in all possible channels

as soon as this is dynamically possible. On the contrary, when the c.m. energy increases, the η production goes down to much lower limits. In fact the η production is low in $p\bar{p}$ annihilation[16]; it goes also down very fast in the reaction $\pi^- + p \rightarrow \eta + n$[17] when the momentum transfer $-t$ goes beyond .3 $(GeV)^2$.

The following of this section is devoted to a quantitative comparison of cross section for π and η production by pions and photons, as a contribute to the understanding of the η-baryon forces, and their influence in the so-called baryon spectroscopy.

B) -Let us start by stressing the following points:

The data on η-production are up to now too scanty to allow a complete phase-shifts analysis, independent from the hints and suggestions coming from the π-N spectroscopy.

The η has in common with the π^0 all the quantum numbers (but isospin and mass), and is in addition assigned to the same octed in SU(3) models (the K, $\bar{K}$, π, η octet[18]). This invites to the hypothesis that the η-N resonances are the same isobaric states of the π-N resonances with branching ratios which may be estimated through SU(3) and phase space[19, 20].

The π-N spectroscopy begins to be rather well known in the 0.5--1.2 GeV region (from π-scattering and π-photoproduction data) and is characterized by π-N resonances.

The diagrams which contribute to η-photoproduction (and probably also to η-production from pions at our energies) are essentially of the type given in fig. 12. They have therefore only nucleons or nucleon

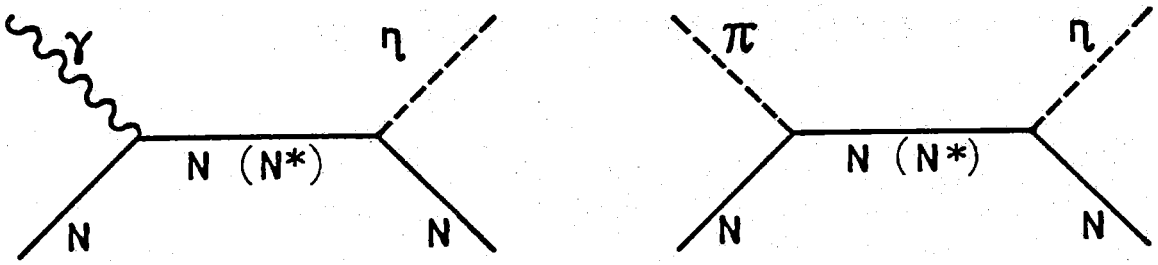

FIG. 12 - Typical graphs contributing to the photoproduction and π-production of η's. N^* stands for an isobaric state of the nucleon.

isobars as propagators (here and in the following, N stands for nucleon, N^* for any excited isobaric state).

In this situation, it seems to us a natural starting point to analyse the η-production data in terms of a comparison with π-production data, in order to determine if the η-N system goes through the same resonances of the π-N system, or if (also) there are peculiar η-N

resonances. We shall see that the second case is probably the right one The comparison must be done between π-N and η-N states with the same isospin and total angular momentum.

To compare the π-N and the η-N systems, let us consider the following cross-sections, and the corresponding reactions with a proton in the initial state

(4a) $\left(\frac{d\sigma}{d\Omega^*}\right)_{\pi^-\eta}$ $\pi^- + p \rightarrow \eta + n$

(4b) $\left(\frac{d\sigma}{d\Omega^*}\right)_{\pi^-\pi^o}$ $\pi^- + p \rightarrow \pi^o + n$

(4c) $\left(\frac{d\sigma}{d\Omega^*}\right)_{\pi^-\pi^-}$ $\pi^- + p \rightarrow \pi^- + p$

(5a) $\left(\frac{d\sigma}{d\Omega^*}\right)_{\gamma\eta}$ $\gamma + p \rightarrow \eta + p$

(5b) $\left(\frac{d\sigma}{d\Omega^*}\right)_{\gamma\pi^o}$ $\gamma + p \rightarrow \pi^o + p$

(5c) $\left(\frac{d\sigma}{d\Omega^*}\right)_{\gamma\pi^+}$ $\gamma + p \rightarrow \pi^+ + n$

and the corresponding total cross sections $\sigma(\pi^-, \eta)$ etc.

We must first separate the different isospin states. Our procedure stays on the following points

- The reaction (π^-, η), (γ, η) are pure $T = 1/2$ states.
- All the other processes indicated in (4), (5) are mixtures of $T = 1/2$ and $T = 3/2$ isospin states.
- It is possible to isolate the $T = 1/2$ isospin in the π scattering: in fact

$$\sigma_{\pi\pi}(T = 1/2) = 3/2 \left[\sigma(\pi^-, \pi^-) + \sigma(\pi^-, \pi^o) - 1/3\ \sigma(\pi^+, \pi^+)\right]$$

- It is not generally possible to isolate the $T = 1/2$ state in π photoproduction, unless we are in a region where $T = 3/2$ is negligible or rather

low. This seems to be our case(x).

With this assumption the relations among the elastic and charge--exchange π cross sections (4) and the photoproduction cross sections (5) become rather simple, and with sufficient approximation we assume:

$$(6) \qquad \sigma_{\pi\pi}(T = 1/2) = \frac{3}{2}\left[\sigma(\pi^-, \pi^-) + \sigma(\pi^-, \pi^0)\right]$$

for the scattering, and:

$$(7) \qquad \sigma_{\gamma\pi}(T = 1/2) = \sigma(\gamma, \pi^0) + \sigma(\gamma, \pi^+) \simeq 3\,\sigma(\gamma, \pi^0)$$

for the photoproduction.

These relations are also valid for the differential cross section, which are indicated as

$$(d\sigma/d\Omega^*)_{\gamma\pi}^{T=1/2} \; ; \; (d\sigma/d\Omega^*)_{\pi\pi}^{T=1/2} \quad \text{etc.}$$

We make now use of these reactions to compare η processes and pion processes in the same isospin state, T = 1/2. In particular we compare the ratios:

$$(8) \qquad R_\gamma(\theta) = \frac{(d\sigma/d\Omega^*)_{\gamma\pi}^{T=1/2}}{(d\sigma/d\Omega^*)_{\gamma\eta}} \simeq 3\,\frac{(d\sigma/d\Omega^*)_{\gamma,\pi^0}}{(d\sigma/d\Omega^*)_{\gamma\eta}}$$

and

(x) - The assumption that in our energy region (800-1000 MeV of the incident γ-ray) the states T = 3/2 give a small contribution, may be rather well justified:
- No resonant state in T = 3/2 seems to play an important role between 1400 and 1800 MeV total mass (that is between 600 and 1200 MeV for the incident photon energy).
- In our energy region the ratio $\sigma(\gamma, \pi^+)/\sigma(\gamma, \pi^0)$ is rather close to 2:1, as predicted for T = 1/2.
- This ratio is close to 2 at 180° of the π, where the contribution of the direct photoproduction term in the π^+ channel is zero. (We thank Prof. C. Schaerf for indicating this point on his data).
- The cross section for π^+ scattering ($\pi^+ + p \longrightarrow \pi^+ + p$) is lower than the corresponding π^- scattering by more than a factor 2[23] in the concerned energy region.

$$R_\pi(\theta) = \frac{(d\sigma/d\Omega^*)^{T=1/2}_{\pi\pi}}{(d\sigma/d\Omega^*)_{\pi\eta}} \simeq \frac{3}{2} \frac{(d\sigma/d\Omega^*)_{\pi^-\pi^-} + (d\sigma/d\Omega^*)_{\pi^-\pi^0}}{(d\sigma/d\Omega^*)_{\pi\eta}}$$

We indicate by R_γ (total) and R_π (total)these ratios when referred to the total cross sections.

The values of R_γ, R_π as a function of the energy are given in fig. 13. We calculated the value of R_γ (120^o) using our measurements for the η, and the results of other authors on the π-photoproduction[21]. R_γ (total) was obtained as $4\pi R_\gamma(\theta)$, this hypothesis being supported by the isotropy of reaction (1) at $\sim$ 800 MeV[13].

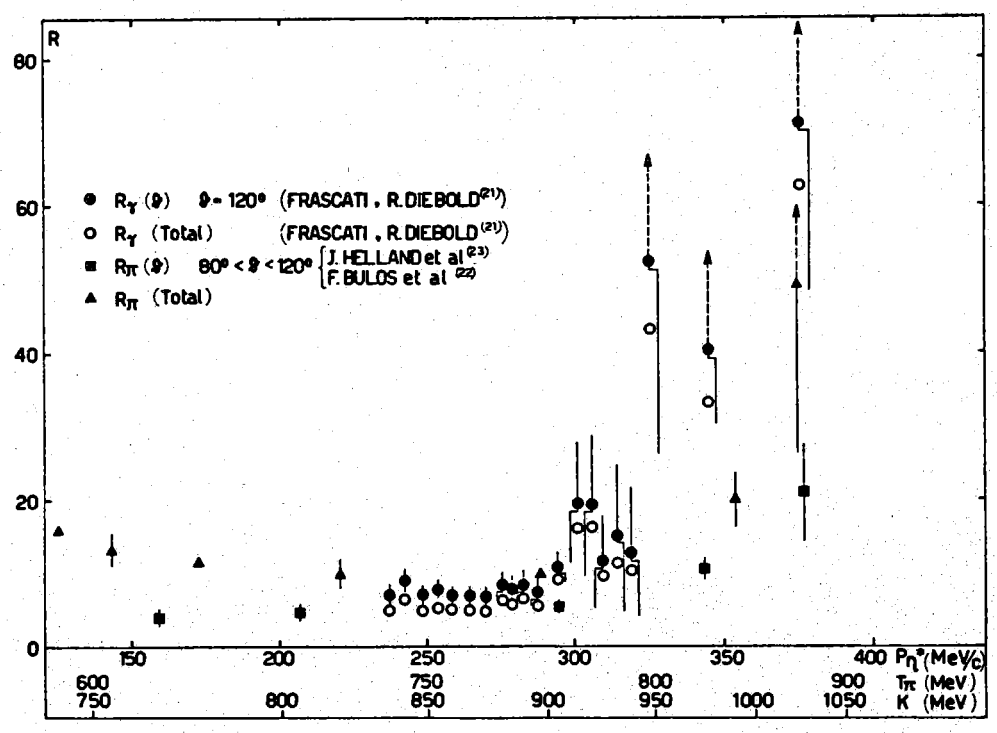

FIG. 13 - The ratio of the π^- to η - production cross-sections, as a function of the c.m. momentum (P^*_η) of the η (upper scale). The laboratory energy of the particle producing the reaction is also reported in the lower scales: kinetic energy of the pion (T_π) and photon energy (K). R_γ and R_π are defined in the text.

The values of $R_\pi(\theta)$ are deduced from the measurements of Bulos et al.[14] on the η, and of the same authors[22] and of J. Helland et al.[23] on the pion exchange and scattering.

The abscissa in fig. fig. 13 is linear with the momentum (P^*_η) of the η in the c.m. system. The angle chosen for $R_\pi(\theta)$ is an average in the interval 80^o - 120^o of the η and the π in the c.m.s. The value R_π (total) is less meaningful, due to the very large contribution of the forward scat

tering in (π^-, π^-) and (π^-, π^o) processes. This large contribution is probably due to the inelastic processes which reflect themselves in the elastic channel as diffraction scattering[23]. Anyway, R_π(total) is reported in fig. 13, and exhibits the same qualitative behaviour than all the other R values shown there.

The R values allow a first quantitative comparison between the π-N and η-N final states. We remark:

a) in the region $140 \leq P^*_\eta \leq 300$ MeV/c the values of R_γ and R_π are rather low, constant, and close in absolute value. This means that the η is rather abundant in this energy interval (one η every 4 or 5 pions); in addition, being $R_\gamma(\theta)$ so close to $R_\pi(\theta)$, the isospin formalism we followed to extract the T = 1/2 state gives results which are remarkably consistent with the experimental evidence.
b) As we go beyond 300 MeV/c of P^*_η, the ratios R increase rapidly to show that pions (from the elastic channels and from single photoproduction) become relatively more abundant with respect to η's.

From these results we could be, at first sight, lead to conclude that the η shares with the pions the second resonance: N^{**} (1512 MeV) $D_{1/2, 3/2}$.

However, following an argument by Dashen[20], the angular momentum factors alone would reduce the contribution of $N^{**}(1512)$ in the η-production by a factor larger than 200 as compared to the π-production. This is very low as compared with the experimental values of R we gave in fig. 13, unless we assume unreasonably high values for the η-N-N^{**} coupling. If any, there is some evidence that the coupling $G(\eta NN^{**}) \simeq .2 G(\pi NN^{**})$[20, 24]. Thus, it is very improbable that the relatively high value of the η photoproduction cross section at 750-850 MeV of the incident photon, can be due to the second resonance(+).

C) - The high value of $(d\sigma/d\Omega^*)_{\gamma\eta}$ at our lowest energies and its fast decrease after 900 MeV (fig. 11) suggests therefore the hypothesis that there is in the η-N system a resonance or an important state which is not so relevant in the π-N system.

This conclusion is not new. In fact the idea that the behaviour of the η-production near threshold is not due to the second resonance, but is rather indicative of an S-wave resonance in the η-baryon system has already been considered by Gyuk and Tuan[26]. More recently Hendry and

---

(+) - Another argument to exclude the second resonance is in the fact that $(d\sigma/d\Omega^*)_{\gamma\eta}$ as well as $(d\sigma/d\Omega^*)_{\pi^-\eta}$ are close to isotropy[13, 14]. A consistent attempt to reconcile isotropy with a dominant $D_{1/2, 3/2}$ state has been done by Altarelli et al[25], when the photoproduction isotropy was still unknown, by interference with an S wave. It is unprobable that the D-S interference works towards isotropy at the same time in the photon and pion input channels.

Moorhouse[19] have examined the situation after the measurements of Bulos et al.[14] and Pauli et al.[27] on the channels:

(10) $$\pi^- + p \rightarrow \eta + n$$

and

(11) $$\pi^+ + n \rightarrow \eta + p$$

They conclude that the sharp linear rise of the cross section as observed in reaction (10), as well as the isotropic c.m. angular distribution up to 800 MeV K.E. of the pion, strongly suggest that the production occurs predominantly in an S-state.

More precisely, the cross section goes approximately linear with the η center of mass momentum, according to the formula for S--wave production:

(12) $$\sigma(\pi + N \rightarrow \eta + N) \propto (\frac{k_2}{k_1}) \left| T_{12} \right|^2$$

where we indicate by 1, 2 the two channels π + N and η +N respectively; $k_1(k_2)$ is the c.m. momentum in channel 1(2); T_{12} is the transition matrix element.

To fix the character of this S-state interaction (that is to look for a resonant behaviour) it is important to examine the development of the cross section values after the rise. Hendry and Moorhouse[19] find that the decrease at higher energies is rather sharp, and seems to require a strong energy variation in the T matrix element. A strong energy variation has likewise been observed in phase shifts analysis of π-N scattering for the $S_{1/2,\,1/2}$ partial wave at energies near the η threshold[28, 29, 30], the behaviour being strongly suggestive of an S-wave resonance in the inelastic channels.

On these suggestions, Hendry and Moorhouse[19] went to a quantitative analysis of channels 1 and 2. They used a multichannel effective range formalism[31] and arrived to the following conclusions:

- There is a good correspondence in energy position between the $S_{1/2,\,1/2}$ in elastic pion nucleon collision (identified by the absorption parameter and its phase shift) and the η production. Notwithstanding, the η production does not fully account for the value of the absorption parameter: a background from one or more channels seems to be necessary.
- When some space is left to the "background" then all the numerical computations tend to individuate the S-state in η production as an $S_{1/2,\,1/2}$ resonance with the following characteristics:

(13) $$E_r = 1519;\ 1505 \text{ MeV}$$
$$\Gamma = 130;\ 77 \text{ MeV}$$

E_r is the effective mass of the η-N resonance, while Γ is its full width. The first values in E_r and Γ come from using the evaluations of Bransden et al.[28] and the second values from Auvil et al.[29].

Now we go back to our results for photoproduction. It is interesting to note that the decrease of the photoproduction cross section with the energy is faster than in the reaction (10), where the η's come from pion beams.

This can be seen in fig. 14, where we report both photoproduction cross section and the cross section of reaction (10).

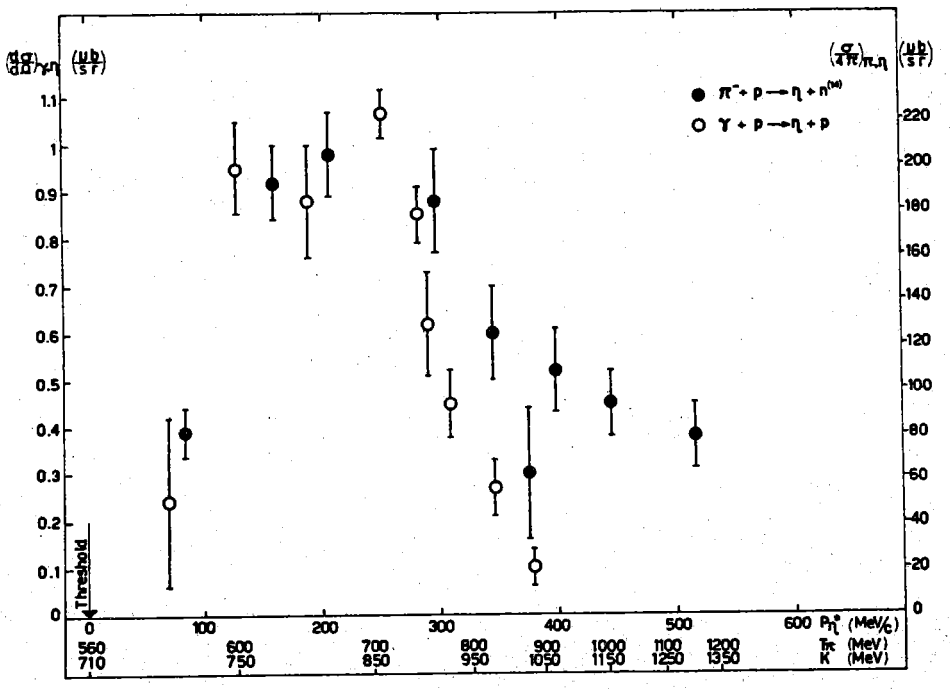

FIG. 14 - Comparison between the cross section of η-photoproduction and η-production by pions[14]. The abscissa is linear in the η c.m. momentum P_η^* (upper scale). In the lower scales the energy (K) of the incident photon and the kinetic energy (T_π) of the incident pion in the laboratory system, are reported. The photoproduction data are to be referred to the left ordinates scale and the π-production data to the right ordinates scale. The photoproduction data are an average of the present results and the results of ref. (13). To get the cross section for η-production from our results and from the results on η production by pions, the measured cross section, referring to the decay mode $\eta \to \gamma\gamma$, was divided by the branching ratio $(\eta \to \gamma\gamma)/(\eta \to$ $\to$ all modes) = 0.38.[12] To give better statistical significance to the comparison we report $\sigma/4\pi$ instead of $d\sigma/d\Omega^*$ for the data on reaction $\pi^- + p \to \eta + n$. $d\sigma/d\Omega^*$ at our angles has the same behaviour as $\sigma/4\pi$, with much larger errors.

The fast decrease of the photoproduction cross section (fig. 11) support the resonance hypothesis with even more immediate evidence than in reaction (10), considering also that, as we said, we already know[13] that the η -photoproduction near threshold is rising at least as fast as the η production by pions, and also has an isotropic angular distribution.

It is possible to make in photoproduction an analysis of the type that Hendry and Moorhouse[19] made using the pion channel, for lack of equivalent information in pion photoproduction. If we try to judge the width of this resonance from the behaviour of the cross section in fig. 11, we find that the possible width of the $S_{1/2,1/2}$ resonance is around 150 MeV a value in agreement with the extimation of Hendry and Moorhouse.[19]

D) - Let's go now to consider the values of $(d\sigma/d\Omega^*)_{\gamma\eta}$ at energies higher than 940 MeV. We have at disposal the points up to 1030 MeV, obtained in this experiment and in the previous work of our group[2][32]. As we said, the cross section for η photoproduction decreases by a factor $\sim$ 5-10 with respect to the value at 830 MeV (fig. 11), and the values of R increase (fig. 13).

It is difficult to assume that this "residual" cross section is a tail of the $S_{1/2,1/2}$ resonance, also considering that in reaction (10) the η cross section is not isotropic at the highest energies, that is beyond $\sim$800 MeV for the pion kinetic energy.

Again, the world information in photo- and pio-production of the η is not enough to try any wave analysis: but this is the region of the well known third resonance (1688 MeV, $F_{1/2,5/2}$; indicated in the following by N^{***}) and one can compare, as before for the second resonance, the values of $(d\sigma/d\Omega^*)_{\gamma\eta}$ and $(d\sigma/d\Omega^*)_{\gamma\pi}$ to see if the production around 1000 MeV of the incident photon could be due to the third resonance.

Following Dashen[20] again, when assuming that the cross sections are completely dominated by the third resonance, one finds:

$$(14) \qquad \frac{(d\sigma/d\Omega^*)_{\gamma\eta}}{(d\sigma/d\Omega^*)_{\gamma\pi^0}} = \frac{G^2(\eta NN^{***})}{G^2(\pi NN^{***})} \cdot \frac{f(q_\eta)}{f(q_\pi)}$$

where $G(\eta NN^{***})$ and $G(\pi NN^{***})$ are the coupling constants of the η and the π respectively, with N and N^{***}; f(q) is a kinematical factor which includes the effects of phase space and angular momentum barrier. One can reasonably estimate $f(q_\eta)/f(q_\pi) \simeq 1/3$. The ratio of the coupling constants is unknown: if N^{***} belongs to an octet representation of SU(3) we have[18][20]

$$(15) \qquad G(\eta NN^{***}) \simeq \frac{1}{\sqrt{3}} (3-4\alpha) G(\pi NN^{***})$$

where α is the ratio of D to F-type couplings.

Relation (14), when the value 1/3 for $f(q_\eta)/f(q_\pi)$ is taken, and the ratio of the cross sections is taken from fig. 11, at K = 980 MeV, becomes:

$$(16) \qquad \frac{G^2(\eta NN^{***})}{G^2(\pi NN^{***})} \leq 3 \frac{(d\sigma/d\Omega^*)_{\gamma\eta}}{(d\sigma/d\Omega^*)_{\gamma\pi^0}} \simeq .15$$

The equality holds in the hypothesis that all the η cross section at 950 - 1000 MeV is due to the N^{***} resonance.

The ratio (16) corresponds, according to (15), to a value of $\alpha \simeq .58$, to be compared with the value $\alpha = .66$ which is generally accepted[28], according to SU(6). This cannot be considered a significant agreement; in fact we are in a critical region: the ratio

$$\frac{G^2(\eta NN^{***})}{G^2(\pi NN^{***})}$$

becomes .037 instead of .15 for $\alpha = 2/3$.

In conclusion, there is enough η production around 1000 MeV to leave just the possible foreseen space to the third resonance. On the other side the energy distributions of reactions (1) and (10) as well as the dependence of R with energy (see for instance R_π (total) in fig. 13) do not indicate any bump or maximum of the cross section in the region of the third resonance.

SECTION 5: CONCLUSIONS -

Our results on the photoproduction cross section of the η in the process $\gamma + p \rightarrow \eta + p$, which are summarized in fig. 11 and in tables II, III allow the following conclusions:

- The η is produced with high abundance at the lowest energies (830-900 MeV of the incident γ), and its cross section has a fast descent in the 900-1000 MeV interval.
- The absolute value of the cross section for photoproduction, and even more clearly the comparison with the photoproduction of the pions, excludes that around 800 MeV the η can be produced through the η-N decay of the second π-N resonance.
- The energy dependence of the cross section from 800 to 1000 MeV of the incident γ, gives instead good support to the hypothesis, already presented on the basis of the results on reactions $\pi + N \rightarrow \eta + N$, that the η is produced near threshold in a $S_{1/2,1/2}$ η-Nucleon resonance, with $E_r \simeq 1520$ MeV, and $\Gamma \simeq 150$ MeV.
- We find a remarkable consistency between the input channels $\pi^- + p$ and $\gamma + p$ at the energies considered here, when the T = 1/2 state is extrac

ted from both channels. In fact the ratios R_γ and R_π (fig. 13) have the same energy dependence, and their absolute values are about equal at each energy. The results agree with the assumption that the reactions (5b) and (5c) are dominated by a T = 1/2 isotopic spin state.
The photoproduction at 950-1050 MeV could be due (or not) to the third resonance: in fact the value of the cross-section at those energies does not disagree with possible SU(3) previsions. It is clear anyway that the majority of the η production which is below 900 MeV of the incident photon energy does not follow the known π-N resonances.

REFERENCES. -

(1) - C. Bacci, G. Penso, G. Salvini, C. Mencuccini and V. Silvestrini, Phys. Rev. Letters 16, 157 (1966) and Phys. Rev. Letters 16, 384 (1966), See also: Proceedings of the International Symposium on Electron and Photon Interactions at High Energies, Hamburg, June 1965.

(2) - C. Bacci, G. Penso, G. Salvini, A. Wattenberg, C. Mencuccini, R. Querzoli and V. Silvestrini, Phys. Rev. Lett. 11, 37 (1963).

(3) - C. Bacci, G. Penso, G. Salvini, A. Wattenberg, C. Mencuccini, R. Querzoli and V. Silvestrini, Laboratori Nazionali di Frascati, Internal Report LNF 64/6 (1964).

(4) - V. Montelatici, Nuclear Inst. and Meth. 29, 121 (1964); and Laboratori Nazionali di Frascati, Internal Report LNF 62/20 (1962).

(5) - C. Bacci, V. Bidoli, G. Salvini and M. Spinetti, Istituto di Fisica, Università di Roma, Internal Report n. 66 (unpublished).

(6) - G. Bologna, G. Diambrini and G. P. Murtas, Suppl. Nuovo Cimento 24, 342 (1962).

(7) - G. Penso and V. Silvestrini, Laboratori Nazionali di Frascati, Internal Report LNF 64/45 (1964).

(8) - M. Rich and R. Madey, U. C. R. L. 2301 (1954).

(9) - G. Diambrini, A. S. Figuera, B. Rispoli and A. Serra, Nuovo Cimento 19, 250 (1961).

(10) - R. R. Wilson, Nuclear Instr. and Meth. 1, 101 (1957).

(11) - G. P. Millburn, W. Birnbaum, W. E. Crandall and L. Schecter, Phys. Rev. 95, 1268 (1954).

(12) - A. H. Rosenfeld, A. Barbaro-Galtieri, W. H. Barkas, P. L. Bastien, J. Kirz and M. Roos, Rev. Mod. Phys. 37, 633 (1965).

(13) - R. Prepost, D. Lundquist and D. Quinn, Eta Photoproduction in the region from threshold to 900 MeV, Proceeding of the International Symposium on Electron and Photon Interactions at High Energies, Hamburg, June 1965.

(14) - F. Bulos, R. E. Lanou, A. E. Pifer, A. M. Shapiro, . M. Widgoff, R. Panvini, A. E. Brenner, C. A. Bordner, M. E. Law, E. E. Ronat, K. Strauch, J. J. Szymanski, P. Bastien, B. B. Brabson, Y. Eisenberg, B. T. Feld, V. K. Fisher, I. A. Pless, L. Rosenson, R. K. Yamamoto, G. Calvelli, L. Guerriero, G. A. Salandin, A. Tomasin, L. Ventura, C. Voci and F. Waldner, Phys. Rev. Letters 13, 486 (1964).

(15) - D. Berley, P. L. Connolly, E. L. Hart, D. C. Rahm, D. L. Stonehill, B. Thevenet, W. J. Willis and S. S. Yamamoto, Phys. Rev. Letters 15, 641 (1965);

- P. L. Bastien, J. P. Berge, O. I. Dahl, M. Ferro-Luzzi, D. H. Miller, J. J. Murray, A. H. Rosenfeld and M. B. Watson, Phys. Rev. Letters 8, 114 (1962).

(16) - C. Baltay, N. Barash, P. Franzini, N. Gelfand, L. Kirsch, G. Lütjens, D. Miller, J.C. Severiens, J. Steinberger, T.H. Tan, D. Tycko, D. Zanello, R. Goldberg and R.J. Plano, Phys. Rev. Letters 15, 532 (1965);
- P. Anninos, L. Gray, P. Hagerty, T. Kalogeropoulos, G. Palomba, S. Zenone, R. Bizzarri, G. Ciapetti, U. Dore, M. Gaspero, G. Gialanella, P. Guidoni, I. Laakso, G. Moneti and G. Natoli, Proceedings of the Second Topical Conference on Resonant Particles, Athens, Ohio, June 1965; See also Proceedings of the LI Conference of the Italian Physical Society, Bologna, November 1965.
(17) - O. Guisan, J. Kirz, P. Sonderegger, A.V. Stirling, P. Borgeaud, C. Bruneton, P. Falk-Vairant, B. Amblard, C. Caversasio, J.P. Guillaud and M. Yvert, Phys. Letters 18, 200 (1965).
(18) - M. Gell-Mann, Phys. Rev. 125, 1067 (1962).
(19) - A.W. Hendry and R.G. Moorhouse, Phys. Letters 18, 171 (1965).
(20) - R.F. Dashen, Nuovo Cimento 32, 469 (1964).
(21) - R. Diebold, Phys. Rev. 130, 2089 (1963).
(22) - F. Bulos et al. (see ref. (14)), Phys. Rev. Letters 13, 558 (1964).
(23) - J.A. Helland, C.D. Wood, T.J. Devlin, D.E. Hagge, M.J. Longo, B.J. Moyer and V. Perez-Mendez, Phys. Rev. 134, B1079 (1964).
(24) - S.L. Glashow and A.H. Rosenfeld, Phys. Rev. Letters 10, 192 (1963); See also ref. (20).
(25) - G. Altarelli, F. Buccella and R. Gatto, Nuovo Cimento 35, 331 (1965).
(26) - I.P. Gyuk and S.F. Tuan, Phys. Rev. Letters 14, 121 (1965).
(27) - E. Pauli, A. Muller, R. Barloutaud, L. Cardin, J. Meyer, M. Beneventano, G. Gialanella, L. Paoluzi and R. Finzi, Proceedings of the Sienna International Conference on Elementary Particles, September 1963, vol. I, pag. 92.
(28) - B.H. Bransden, P.J. O'Donnel and R.G. Moorhouse, Phys. Letters 11, 339 (1964); Rutherford Lab. Report NIRL/R/79.
(29) - P. Auvil, C. Lovelace, A. Donnachie and A.T. Lea, Phys. Letters 12, 76 (1964).
(30) - L.D. Roper, Phys. Rev. Letters 12, 340 (1964);
- L.D. Roper and R.M. Wright, UCRL 7846 (1964).
(31) - M.H. Ross and G.L. Shaw, Ann. of Phys. 9, 391 (1960); 13, 147 (1961);
- R.H. Dalitz, Ann. Rev. Nucl. Sci. 13, 339 (1963).
(32) - C. Bacci, G. Penso, G. Salvini, A. Wattenberg, C. Mencuccini, R. Querzoli and V. Silvestrini, Proceedings of the Conference on Photon Interactions in the BeV-Energy Range, Cambridge, Mass. Jan. 1963, pag. IV.6.
(33) - B. Delcourt, J. Lefrançois, J.P. Perez Y Jorba and J.K. Walker, Phys. Letters 7, 215 (1963).